

Tin-vacancy complexes in silicon

M. Kaukonen and R. Jones

School of Physics, University of Exeter, Exeter EX4 4QL, United Kingdom

S. Öberg

Department of Mathematics, Luleå University of Technology, SE-97187 Luleå, Sweden

P. R. Briddon

Department of Physics, University of Newcastle upon Tyne, Newcastle upon Tyne NE1 7RU, United Kingdom

(Received 26 February 2001; revised manuscript received 16 July 2001; published 10 December 2001)

The structure and electrical properties of SnV_2 , Sn_2V , and Sn_2V_2 complexes in Si are investigated using first-principles cluster and supercell methods. The formation of SnV_2 and Sn_2V_2 is found to be energetically favorable, in agreement with the experimental results. All the tin-vacancy defects are found to possess deep donor and acceptor levels, although the number of the gap states decreases with increasing size of the defect. The diffusion of tin in silicon is considered and the mechanism found to be distinct from the diffusion of group V shallow donors. In contrast with these, the Sn-V interaction is found to extend only to the third nearest neighbor distance. This implies that the activation energy for Sn diffusion via vacancies should be nearly the same as self-diffusion by this mechanism. We find an activation energy of 3.5 eV which is close to some experimental findings but considerably less than given by others.

DOI: 10.1103/PhysRevB.64.245213

PACS number(s): 66.30.Jt, 61.72.Bb, 61.72.Ji, 61.80.Az

I. INTRODUCTION

Vacancies in silicon are important radiation defects which possess deep electrical levels.¹ The single vacancy in silicon is not stable at room temperature. It becomes mobile at 70 K (*n*-type silicon) or at 150 K (*p*-type silicon) and readily complexes both with other vacancies creating multivacancy centers, as well as with many impurities.² The divacancy introduces acceptor levels in the upper half of the band gap: a single ($-/0$) level at $E_c - 0.4$ eV and a second acceptor level at $E_c - 0.2$ eV.³ Similarly, the vacancy-oxygen center introduces a single acceptor level at $E_c - 0.17$ eV.⁴ However, vacancies are not only important in introducing deep electronic levels but as complexes with impurities they can promote impurity diffusion.⁵ For example, shallow dopants such as arsenic diffuse by complexing with vacancies forming AsV. The resulting defects moves through the lattice as a complex with a migration energy ~ 1.2 – 1.4 eV somewhat less than the dissociation energy of the defect.^{6,7}

Early work on tin doped Si (Ref. 9) found that vacancies are readily trapped by tin, in preference to oxygen,¹⁰ leading to an SnV center which is stable up to ~ 400 K in the temperature region when divacancies are formed. Until recently, the only electrical levels correlated with the defect were single and double donor levels lying in the lower half of the band gap¹¹ at $E_v + 0.32$, $E_v + 0.07$ eV, respectively. This has led to suggestions that tin doped *n*-Si would be a radiation hard material as any SnV defects formed might be electrically inactive in *n*-Si. However, this electrical inactivity is not a valid assumption.

The SnV defect is magnetically active and the G29, $S = 1$, electron paramagnetic resonance (EPR) center having D_{3d} symmetry has been assigned to the neutral defect.¹² In this center the tin atom is located in the middle of a divacancy. We have investigated the SnV center earlier¹³ finding

both its structure and electrical levels. It was found that the neutral defect has D_{3d} symmetry—in agreement with experiment—and remarkably that the center possesses five charge states and thus can act as a deep single and double acceptor as well as a single and double donor. At the same time,¹³ deep level transient spectroscopic (DLTS) experiments have found these acceptor levels at $E_c - 0.5$, and $E_c - 0.21$ eV. Other workers report similar levels.^{15,16}

The SnV defect is not, however, the only Sn related radiation center. In heavily *e*- irradiated *n*-Si, EPR experiments¹⁷ have shown that a new Sn related spin 1/2 center called DK1 is present. The latter has been assigned to $(\text{SnV}_2)^-$. This defect anneals around 500 K and two new EPR centers DK2 and DK3 are then formed. These have been associated with two different configuration of $(\text{Sn}_2\text{V}_2)^-$. The EPR experiments unambiguously showed that each contains two equivalent tin atoms and DK2 possesses C_{2h} symmetry while the symmetry of DK3 is C_{1h} .

These $(\text{Sn}_2\text{V}_2)^-$ defects disappear at 690 K—well above the temperature where V_2 defects are stable. Thus it appears that tin can stabilize vacancy centers. Although many details about these defects have been uncovered by EPR, their electrical levels are at present unknown.

There is uncertainty over the activation energy of diffusion of Sn in Si. The experimental evidence suggests that it proceeds by a vacancy mediated mechanism. However, it is not clear whether the mechanism is the same as for the *E*-center.^{18,5} In this mechanism the vacancy escapes from a site neighboring an impurity atom and travels around a hexagonal ring of Si neighbors before returning to complex with the impurity in a different orientation. Finally, the impurity and vacancy are interchanged.

The activation energies for Sn diffusion in Si found by different groups are quite scattered. Akasaka *et al.*¹⁹ investigated the diffusion of tin introduced from a tin-doped oxide

using Rutherford backscattering and channeling. They found more than 90% of Sn atoms lay at substitutional sites, and the tin solubility is $\sim 0.01\%$ at 1100–1200 °C. They also reported a diffusion energy, 3.5 eV, for tin. Yeh *et al.*²⁰ used neutron activation analysis to determine the diffusion of Sn finding a barrier of 4.25 eV.

Secondary-ion mass spectrometry (SIMS) measurements were made by Kringhøj *et al.*²¹ to determine the diffusion of tin in δ -doped molecular beam epitaxy (MBE) grown samples. They demonstrated that the injection of vacancies enhanced tin diffusion implying a vacancy mechanism, and reported a diffusion barrier of 4.8 eV which is considerably greater than given earlier.

In this paper, we extend our earlier studies of the structure

and electronic levels of tin-vacancy centers to investigate SnV_2 , Sn_2V , and Sn_2V_2 defects as well as exploring the diffusion and reorientation of SnV . We utilize an *ab initio* density functional method (AIMPRO) employing large hydrogen terminated clusters (~ 300 atoms) as well as supercells. In this study we use clusters only for the determination of the electronic levels and for the wave function plots. All the the total energy calculations (i.e., formation, migration and reaction energies) are done in supercells. Supercells have the advantage of giving converged energies for defects irrespective of their location within the supercell, but clusters are useful both for their speed and for the evaluation of electrical levels. Both methods use a basis of Gaussian orbitals and they principally differ in the treatment of the charge

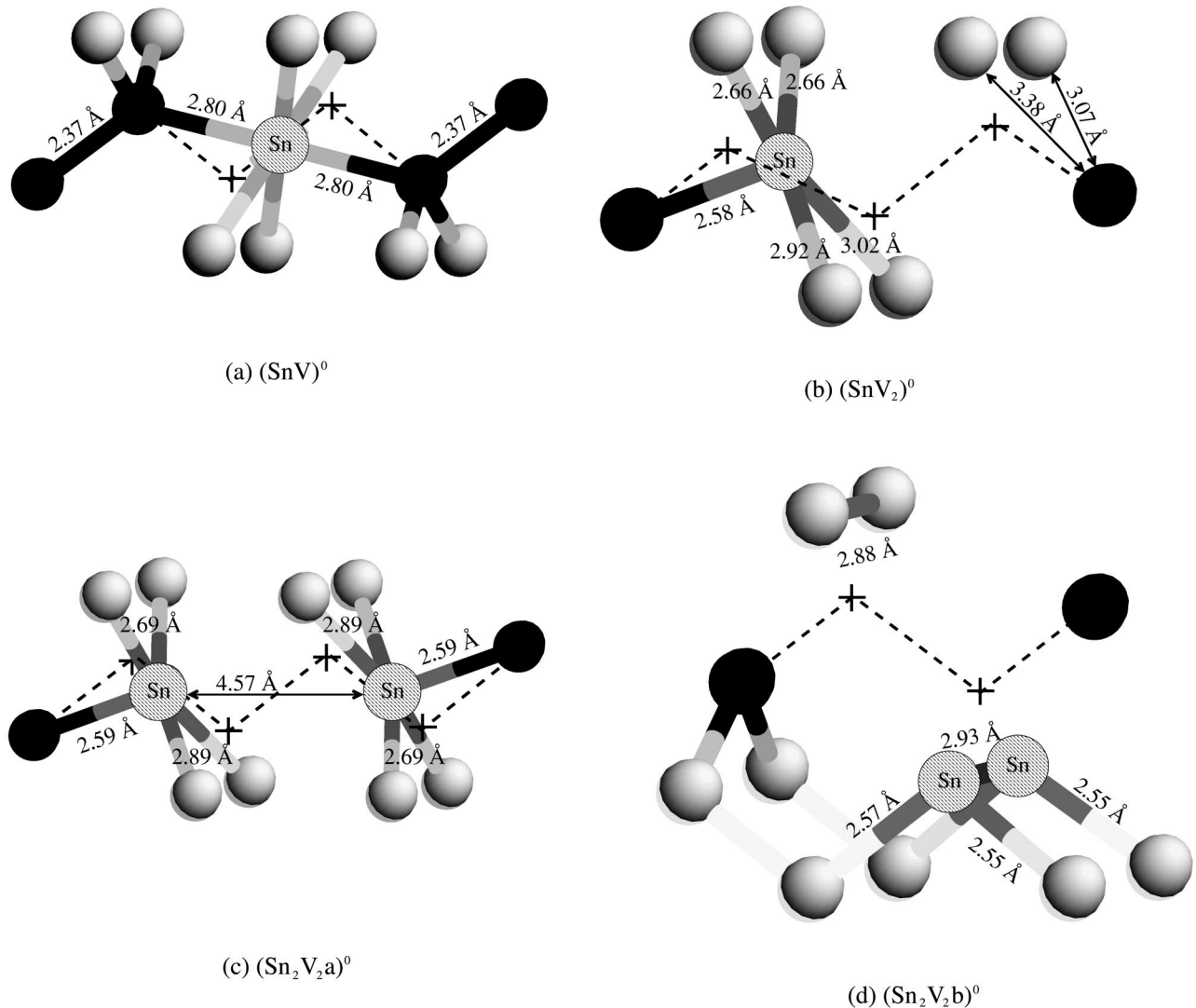


FIG. 1. The schematic structure of $(\text{SnV})^0$, $(\text{SnV}_2)^0$, $(\text{Sn}_2\text{V}_2a)^0$, and $(\text{Sn}_2\text{V}_2b)^0$ defects. The vacancies are indicated with crosses. The original $[110]$ chain is shown with dotted lines. The black atoms are Si atoms on the same $(1\bar{1}0)$ plane as the Sn atom(s) (except in $(\text{Sn}_2\text{V}_2b)^0$). White spheres represent Si atoms in the two neighboring $(1\bar{1}0)$ planes. The $(\text{SnV})^0$ center has D_{3d} symmetry. Sn is bonded to six Si atoms with equal bond lengths of 2.80 Å. The $(\text{SnV}_2)^0$ has C_1 symmetry, the Sn atom has moved towards the divacancy on the $(1\bar{1}0)$ plane. The C_{1h} symmetry is broken by the movement of the four silicon atoms with dangling bonds on the opposite sides of the $(1\bar{1}0)$ plane. The $(\text{Sn}_2\text{V}_2a)^0$ center has C_{2h} symmetry. The two Sn atoms remain on the $(1\bar{1}0)$, each moving towards the central divacancy. The $(\text{Sn}_2\text{V}_2b)^0$ center has C_{1h} symmetry. A reconstructed Sn-Sn bond is formed with the length of 2.93 Å.

density. In the cluster method this is expanded in a set of Gaussian functions while a Fourier series is used in the supercell. In the cluster calculations the wavefunctions were expanded in a basis consisting of N Cartesian s , p Gaussian orbitals sited on each atom. The charge density was fitted to M Gaussian functions. In this study, (N, M) were (6,6) for Sn, (4,5) for Si, and (2,3) for H. Two extra Gaussian orbitals with different exponents, located midway between each bonded pair of atoms (excluding the H terminators), were added to the wave function basis, and similar bond centered functions were added to the basis for the charge density. In the supercell calculations only atom centered Gaussians were utilized with additional four exponential functions for Si each combined with s , p and d orbitals yielding totally 36 functions/atom. For Sn six exponentials were used. For the two most diffuse exponents s , p , and d functions were used and for the for four others s , p angular functions only summing up to 34 functions/atom. Additional details of the methodology are found in Refs. 22,23. We employ Bachelet-Hamann-Schlüter pseudopotentials^{24,25} with four valence electrons for both Si and Sn. For the supercell calculations, the total energies of tin centers were calculated in a ~ 64 atom supercell containing the defect with $2 \times 2 \times 2$ Monkhorst-Pack k -point sampling.^{26,27} The calculations were repeated using larger ~ 216 atom cells at the Γ point. We believe the calculated reaction energies based on the energy differences of similar defects are accurate ~ 0.3 eV as evidenced by the calculated solubility of Sn in Si to be discussed below. However, because of the computational limitations, we have not been able to complete proper convergence tests with respect to the size of the supercell.

Section II gives details of the structures of tin-vacancy defects while Sec. III discusses their electronic levels. In Sec. IV the energetics of tin-vacancy complexes as well as the solubility of tin in silicon are reported and finally we discuss the diffusion of Sn in Sec. V. Our conclusions are given in Sec. VI.

II. THE SnV_2 , Sn_2V , AND Sn_2V_2 DEFECTS

The schematic geometries of the calculated neutral $(\text{Sn}_x\text{V}_x)^0$ centers are shown in Fig. 1. For completeness we have included also $(\text{SnV})^0$ which has been studied earlier.¹³

Room temperature electron irradiation of tin doped n -Si produces the G29 EPR center assigned to the $S=1$ neutral SnV defect and additionally a weaker signal arising from SnV^- (DK4).¹⁷ These anneal out at ~ 430 K with the simultaneous formation of V_2^- and a new $S=1/2$ EPR center called DK1.¹⁷ This center has C_{1h} symmetry around 40 K but C_1 around 8 K. Hyperfine interactions with a single Sn nucleus, and four shells of Si neighbors are resolved by EPR. The tensors related to Si all display trigonal symmetry suggesting dangling bonds. The spin density on Sn is about 50% of that on Sn in G29 as estimated from the ratio of their hyperfine tensors. The spin density on a single Si atom lying in the mirror plane is about a third of that on the pair of dangling bond atoms in V_2^- , while that on a shell of two Si neighbors out of the mirror plane is somewhat greater. The model proposed for DK1 is the $(\text{SnV}_2)^-$ defect shown in

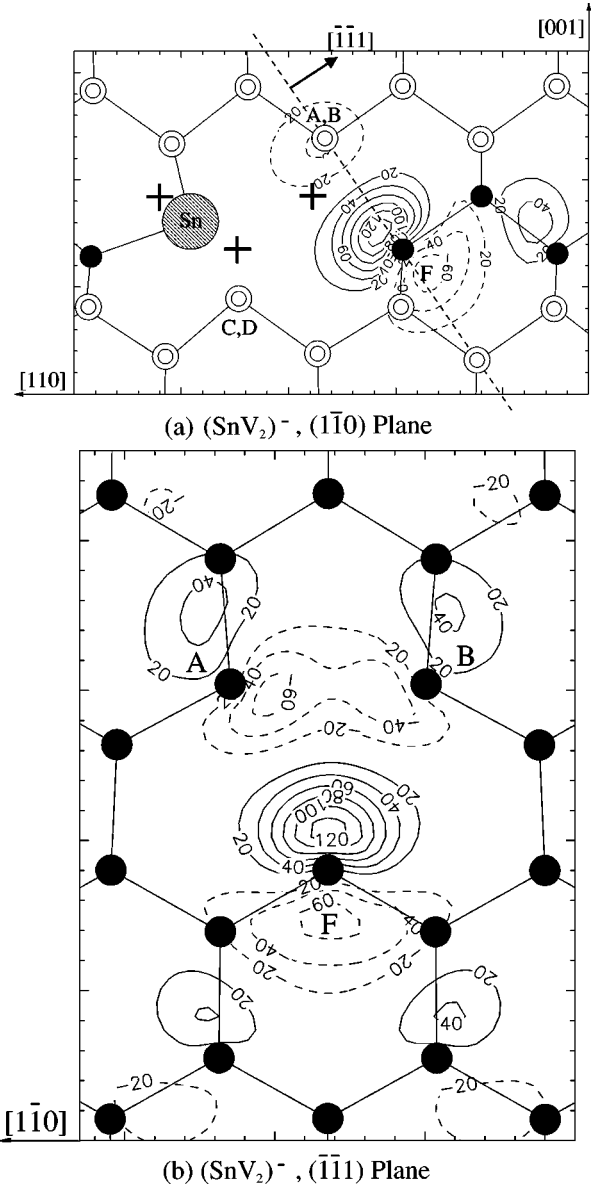


FIG. 2. The structure of $(\text{SnV}_2)^-$. The Sn atom remains near the substitutional site. It and the black Si atoms lie in the $(\bar{1}\bar{1}0)$ mirror plane. The two Si atoms above and below the $(\bar{1}\bar{1}0)$ plane are marked with concentric open circles. The unpaired wave function projected onto the $(\bar{1}\bar{1}0)$ plane is localized in dangling bonds on atoms F , A , and B . Labels are given in units of $10^{-3}\sqrt{\text{electrons/a.u.}^{-3/2}}$.

Fig. 2. It is suggested that Sn lies slightly outside the mirror plane at low temperatures but, at 40 K, it can tunnel, or hop, between the two equivalent sites above and below the plane effectively resulting in C_{1h} symmetry.¹⁷

Calculations carried out in ~ 64 and ~ 216 atom supercells found that the $(\text{SnV}_2)^-$ center shown in Fig. 2 is stable but without any tendency for the Sn atom to move out of the $(\bar{1}\bar{1}0)$ mirror plane. The tin atom is displaced about 0.8 Å from its lattice site along $[112]$ direction. The Sn-Si bond lying in the mirror plane is 2.58 Å, and the pair directed out of this plane are 2.67 Å. The same structure was found by

starting from a planar trivacancy V_3 into which a Sn atom was inserted midway between two vacant lattice sites along $[110]$. Additionally, the Sn atom relaxed back to the mirror plane when initially displaced away. However, we find the distortion from C_{1h} to C_1 symmetry, by a reconstruction of the dangling Si bonds. In Fig. 2(a) one of the Si atoms C (or D) moves slightly closer to Sn compared with the other one ($\text{Sn-Si}_C = 3.98 \text{ \AA}$, $\text{Sn-Si}_D = 3.93 \text{ \AA}$). More importantly, a Si atom A (or B) clearly moves closer to the Si atom F ($\text{Si}_F\text{-Si}_A = 3.10 \text{ \AA}$, $\text{Si}_F\text{-Si}_B = 3.39 \text{ \AA}$, and $\text{Si}_A\text{-Si}_B = 3.36 \text{ \AA}$). This result is consistent with the observation of C_1 symmetry at low temperatures.¹⁷ The same C_1 symmetry is found for $(\text{SnV}_2)^0$ and shown in Fig. 1.

The wave function of the unpaired electron in $(\text{SnV}_2)^-$, in the $(1\bar{1}0)$ mirror plane and in the $(\bar{1}\bar{1}1)$ plane, are shown in Fig. 2. The spin density is almost zero near tin and is mainly localized on the three Si atoms with dangling bonds (A, B , and F) and the neighbors to F .

Although the lack of a spin density on Sn is in agreement with DK1, its high value on the atom F possessing a dangling bond is at variance with the experimental data. The small spin densities found on atoms A, B, C , and D are, however, consistent with experiment.

Annealing the irradiated material to $\sim 500 \text{ K}$ removes $(V_2)^-$ (G7) and $(\text{SnV}_2)^-$ (DK1) and two new $S = 1/2$ centers, labeled DK2 and DK3, are formed. The intensity of DK2 is increased by illumination whereas that of DK3 is unaffected. The new centers have C_{2h} and C_{1h} symmetry, respectively. Hyperfine interactions with two equivalent Sn atoms were resolved for each defect.

In DK2, the Sn atoms are connected by inversion symmetry and a model has been proposed based on two Sn atoms lying at sites bordering a divacancy.²¹ This $(\text{Sn}_2V_2a)^-$ defect is shown in Fig. 3. DK3 is then suggested as an alternative structure $(\text{Sn}_2V_2b)^-$ shown in Fig. 4.

Our calculations found that the $(\text{Sn}_2V_2a)^-$ shown in Fig. 3 is stable and has C_{2h} symmetry in agreement with the DK2 EPR center. The two Sn atoms relax slightly in the $(1\bar{1}0)$ plane, each moving 0.8 \AA along $[112]$ and $[1\bar{1}\bar{2}]$ directions. The Sn-Si bonds in the mirror plane are 2.58 \AA , while those directed out of the plane are 2.67 \AA , essentially the same lengths as found for $(\text{SnV}_2)^-$ above. The bonds of the four undercoordinated Si atoms A_1, B_1, A_2, B_2 in Fig. 3, have lengths deviating less than 0.05 \AA from those of bulk Si (2.34 \AA). Figure 3 shows that the unpaired wavefunction is nodal in the $(1\bar{1}0)$ mirror plane and is localized on the 12 Si atoms lying outside this plane consistent with the EPR data.

DK3 has been assigned to the second form of the double tin-double vacancy $(\text{Sn}_2V_2b)^-$ shown in Fig. 4. We find this has energy 0.4 eV higher than the C_{2h} form. This energy difference makes it unlikely that roughly equal numbers of $(\text{Sn}_2V_2a)^-$ and $(\text{Sn}_2V_2b)^-$ should be formed when DK1 anneals if thermal equilibrium was achieved. However, as experiment indicates otherwise, it suggests that SnV_2 diffuses to Sn and forms both conformations of $(\text{Sn}_2V_2)^-$ but the barrier to interconversion is too high at 500 K for equilibrium to be achieved. Figure 4 shows that the $(1\bar{1}0)$

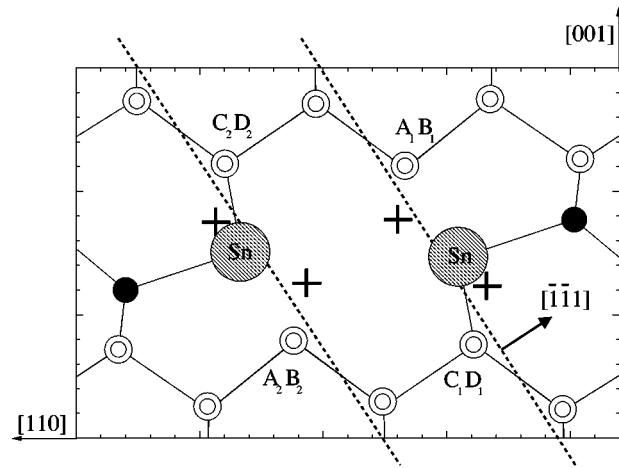
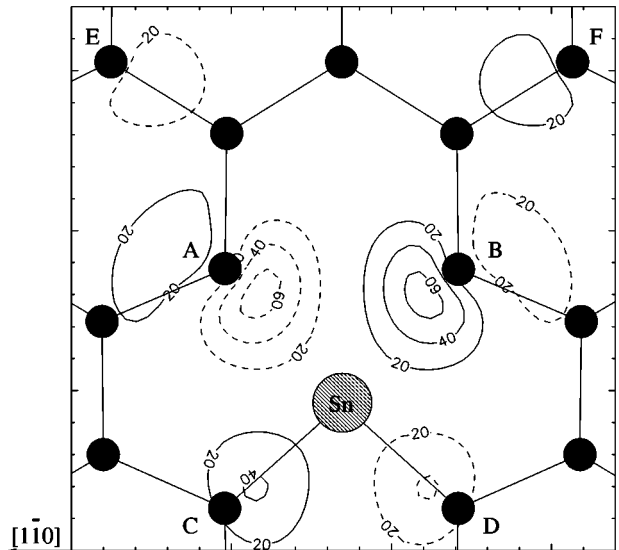
(a) $(\text{Sn}_2V_2a)^-$, $(1\bar{1}0)$ Plane(b) $(\text{Sn}_2V_2a)^-$, $(\bar{1}\bar{1}1)$ Plane

FIG. 3. $(\text{Sn}_2V_2a)^-$ (DK2): The tin atom and the black Si atoms lie in the $(1\bar{1}0)$ mirror plane with two Si atoms lying above and below this plane (open circles). The unpaired wave function is nodal in this plane and localized on the 12 Si atoms symmetrically related to A, B, C, D, E , and F . The right hand figure shows the wave function in the $(\bar{1}\bar{1}1)$ plane (indicated by dotted lines in the left hand figure). The wave function has equal amplitude on the both $(\bar{1}\bar{1}1)$ planes (these planes are related via the C_2 symmetry operation). Labels are given in units of $10^{-3} \sqrt{\text{electrons/a.u.}}^{-3/2}$.

mirror plane is again a nodal surface for the unpaired wave function. The spin is now localized in the dangling bond orbitals of the Si atoms A and B lying out of the plane.

Finally we investigated the structure of Sn_2V . This defect is constructed by replacing two Si neighbors of a vacancy by Sn. The other pair of Si neighbors do not reconstruct. The Sn-Sn distance is 3.0 \AA and the two Si atoms with dangling bonds relax towards the vacancy $\approx 0.2 \text{ \AA}$. The C_{2v} symmetry of the defect rules it out as a candidate for DK3.

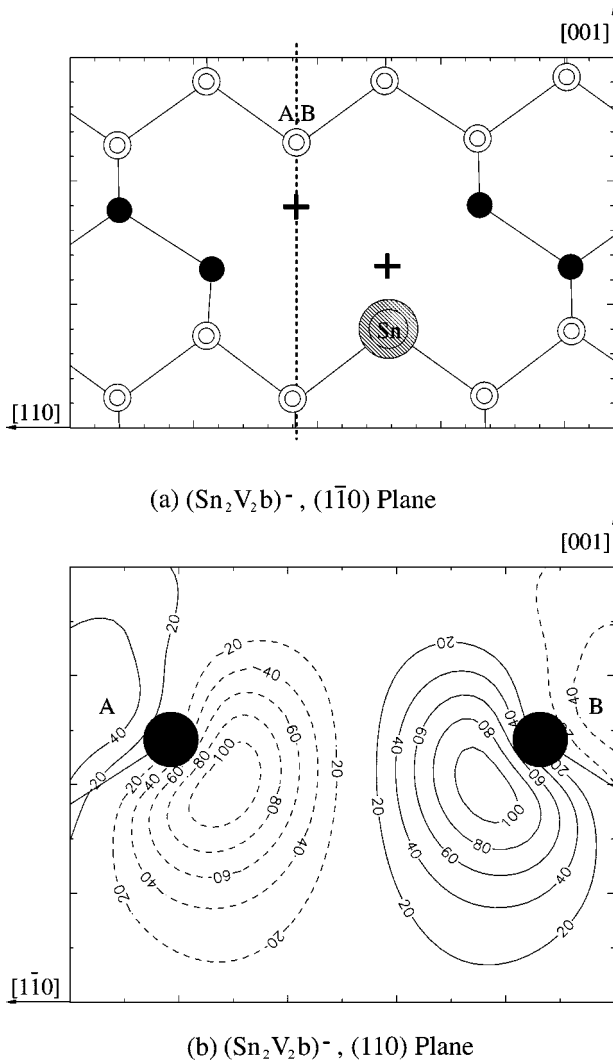


FIG. 4. $(\text{Sn}_2\text{V}_2\text{b})^-$ (DK3): The Sn atoms lie above and below the $(1\bar{1}0)$ mirror plane. The unpaired wave function is shown in the plane through A, B and two other Si atoms and is localized to the dangling bonds on atoms A and B. The function is nodal on the mirror plane. Labels are given in units of $10^{-3}\sqrt{\text{electrons/a.u.}}^{-3/2}$.

III. ELECTRONIC LEVELS

The electronic levels are obtained using clusters having ~ 300 atoms. The donor (acceptor) level of a defect with respect to a standard defect is found by comparing the calculated ionization energies (electron affinities) of the defect, I_d , with that of a standard defect I_s . Thus $E(0/+)_\text{rel} = E(0/+)_d - E(0/+)_s = I_s - I_d$ (Fig. 5). The level with respect to the band edge is then obtained by adding the experimental value of the energy level of the standard defect. In practice the ionization energies and electron affinities are found using Slater's transition state method.^{28,29}

The standard defects used are substitutional Pt, the carbon interstitial C_i , and the AuH_1 center. The second donor level of Pt lies at $E_v + 0.07$ eV,³⁰ while the single donor and acceptor levels of C_i are $E_v + 0.28$ and $E_c - 0.1$ eV, respectively.³¹ The second acceptor level of AuH_1 is taken to lie at $E_c - 0.19$ eV.^{32,33}

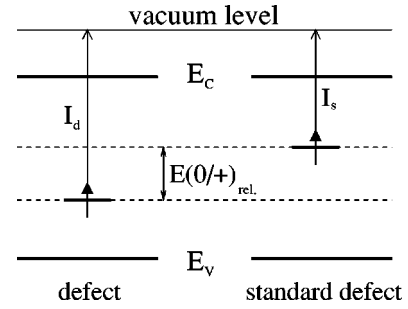


FIG. 5. The donor (acceptor) energy level is obtained by comparing the calculated ionization energy (electron affinity) I_d^calc to the calculated ionization energy (electron affinity) of a standard defect I_s^calc for example, $E(0/+)^\text{rel}_d = I_s^\text{calc} - I_d^\text{calc}$. In this example, one obtains the position of the defect level $E(0/+)^\text{rel}_d$ with respect to the standard defect. The position of the level with respect to the band edges is found by adding the experimental level of the standard defect $E(0/+)^\text{exp}_s$.

The Kohn-Sham levels of the tin-vacancy aggregates are shown in Fig. 6 and Table I gives the energy levels including those of SnV published earlier.¹³ The SnV_2 defect has levels slightly above those of SnV . Unlike SnV_2 , Sn_2V_2a does not possess a second acceptor level. This is because its HOMO wave function for the negative charge center is less localized than the corresponding one in SnV_2 (Figs. 2 and 3). The EPR experiments demonstrate that these centers have deep single acceptor levels as found here, but they have not so far been observed by DLTS. This is probably because the high vacancy concentrations required to form the di-tin species render the diodes insulating. In Sn_2V , the unreconstructed broken bonds gave deep single and double acceptor levels at $E_c - 0.60$ and $E_c - 0.25$ eV. It is seen that the error in the calculated levels of this defect are around ± 0.2 eV. The spin densities of SnV^- , SnV^0 ($S=1$), and SnV^+ are localized on the six neighboring Si atoms, in contrast with the case of the divacancy V_2^- or V_2^+ where two pairs of Si dangling bonds reconstruct.¹⁴

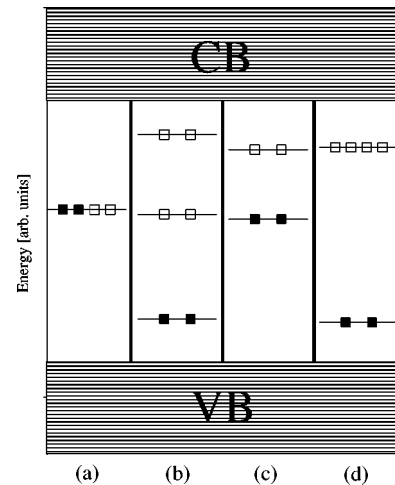


FIG. 6. The calculated one-electron levels of the tin-vacancy related centers. (a) SnV , (b) SnV_2 , (c) Sn_2V , and (d) Sn_2V_2a .

TABLE I. The calculated electronic levels of the multitin-multivacancy defects. The experimental values for SnV are given in parenthesis. The acceptor levels [(=/-), (-/0)] are given with respect to the edge of the conduction band minimum and the donor levels [(0/+), (+/+)] with respect to the edge of the valence band maximum. All the values are in eV.

	(=/-)	(-/0)	(0/+)	(+ / +)
SnV	0.39 (0.21) ^a	0.56 (0.50) ^a	0.22 (0.32-0.35) ^{b,c}	0.09 (0.07) ^c
SnV ₂	0.17	0.53	0.25	
Sn ₂ V	0.25	0.60	0.13	
Sn ₂ V _{2a}		0.38	0.16	

^aReference 21.

^bReference 12.

^cReference 11.

IV. FORMATION AND REACTION ENERGIES

The formation energies of neutral vacancy-tin defects are calculated using the standard formula

$$E_f = E_D - \sum_s n_s \mu_s, \quad (1)$$

where E_D is the total energy of the supercell containing the defect, n_s is the number of atoms of species s and μ_s is the chemical potential of atom species s .^{34,35} μ_{Si} is the chemical potential of a Si atom (i.e., the total energy / Si atom in bulk silicon calculated in a two-atom supercell). The chemical potential for Sn, μ_{Sn} , was calculated using gray tin (i.e., α tin) which also has the diamond structure, which is the stable low temperature form of the element. The reaction energies are obtained by subtracting the formation energies of the initial compounds from those of the products.

Table II gives the formation energies of the tin-vacancy defects. The energy difference between a Sn atom in gray tin and the substitutional defect in Si is 0.5 eV. This would imply that the *equilibrium* concentration of dissolved tin in Si, when in contact with a metallic tin source, is $5 \times 10^{22} e^{-0.5 \text{ eV}/kT} \text{cm}^{-3}$, or $\sim 1.5\%$ at 1100 °C, neglecting

TABLE II. The formation energies of the tin-vacancy related defects in silicon. The reference structure for Si is bulk-silicon and for Sn α -tin (these are calculated in 2 atom diamond cell with $6 \times 6 \times 6$ MP sampling). The calculations are done in 216- X atomic supercells at the Γ point, the numbers in the parenthesis refer to 64- X atom cell calculations with $2 \times 2 \times 2$ MP sampling. All values are in eV.

Complex	Formation energy
Sn	0.5
V	3.3 (3.4)
V ₂	5.0 (5.7)
SnV	2.8 (2.7)
SnV ₂	4.6 (5.2)
Sn ₂ V	2.9 (2.6)
Sn ₂ V _{2a}	3.9 (4.4)

TABLE III. The reaction energies of the tin-vacancy related reactions. A negative value indicates that energy is lowered when moving to the direction of the arrow, i.e., the reaction is exothermic. The calculations are done in 216- X atomic supercells at the Γ point, the numbers in the parenthesis refer to 64- X atom cell calculations with $2 \times 2 \times 2$ MP sampling. All values are in eV.

Reaction	Reaction energy
Sn + V \rightarrow SnV	-1.0(-1.2)
V + SnV \rightarrow SnV ₂	-1.5(-0.9)
V + SnV \rightarrow V ₂ + Sn	-0.6(+0.1)
V ₂ + Sn \rightarrow SnV ₂	-0.9(-1.0)
V + V \rightarrow V ₂	-1.6(-1.1)
Sn + SnV \rightarrow Sn ₂ V	-0.4(-0.6)
SnV ₂ + Sn \rightarrow Sn ₂ V _{2a}	-1.2(-1.3)
SnV + SnV \rightarrow Sn ₂ V _{2a}	-1.7(-1.0)
Sn ₂ V + V \rightarrow Sn ₂ V _{2a}	-2.3(-1.6)
Sn ₂ V _{2a} \rightarrow Sn ₂ V _{2b}	+0.5(+0.4)

any vibrational entropic effects. Experimentally, the solubility of Sn in Si when introduced from an oxide source is $\sim 0.14\%$ at 1100–1200 °C (Ref. 19) corresponding to a formation energy of around 0.8 eV. We suppose that the difference either arises from the lower chemical potential of tin in the oxide compared to our idealized case where the tin source is gray tin³⁵ or the formation energy is underestimated by 0.3 eV.

The formation energies of the tin-vacancy centers are all much greater than that of substitutional tin implying that the dominant tin species is the substitutional defect and that the equilibrium thermal concentration of the former is negligible. Appreciable concentrations of tin vacancies can only arise when a non-equilibrium concentration of vacancies is introduced by, for example, electron irradiation. However, the diffusion of tin appears to be controlled by a thermally generated tin-vacancy defect.

The calculated reaction energies for the various neutral tin-vacancy defects are given in Table III. The vacancy is bound to Sn with an energy of 1.0 eV. This is comparable with the binding energies in OV [1.6 eV (Ref. 23)], PV [1.05 eV (Ref. 18)] and AsV [1.2–1.3 eV (Refs. 6,7)]. A second vacancy is bound to SnV with a higher energy of 1.5 eV.

The anneal of SnV₂ leads to the formation of Sn₂V_{2a} and Sn₂V_{2b}. The binding energy of V with Sn₂V_{2a} is 2.3 eV accounting for the higher thermal stability of Sn₂V_{2a} when compared with SnV. Experimentally Sn₂V₂ is stable until 690 K. The slightly higher calculated binding energies for the neutral SnV₂ and Sn₂V_{2a} than expected based on the experimental annealing temperatures may arise if the dissociation products are charged.

An interesting possibility not considered previously is that mobile SnV are trapped by Sn. However, the binding energy ~ 0.4 eV is lower than the migration energy of SnV and thus Sn₂V is unlikely to form. This is consistent with experiment which do not report any center attributed to (Sn₂V)⁻.

For the charged defects the reaction energies of Table III change because of the Fermi-level effect.⁵ For example, for single and double negative charge states the reaction Sn

+ V \rightarrow SnV becomes less favorable because electrons have to occupy higher levels in SnV compared with V.⁸ We estimate reaction energies of -0.8 and -0.5 eV for singly and doubly negative defects, respectively. The opposite is true for SnV⁺ and SnV⁺⁺, as the reactions then become more exothermic with energies -1.1 and -1.2 eV for singly and doubly positive defects. Generally speaking, the largest effect of the charge on the reaction energies of Table III are in the cases when a (doubly) negatively charged vacancy occurs in the reaction (rows 1, 2, 3, 5, and 9 in Table III, and the reactions become then less favorable from left to right). In other cases the Fermi-level effect is less prominent because of the defect levels of the reactants and products are closer each other.

V. DIFFUSION OF TIN

Impurities generally diffuse either by a direct exchange with Si neighbors, or by complexing with a vacancy or interstitial. In many cases all three mechanisms contribute. Experimental studies involving Sn and Sb δ -doped epi-Si demonstrate that the diffusivities of both impurities increases by a factor of 5 at 1000 °C under the injection of vacancies.²¹ This is taken to indicate that both impurities diffuse by a vacancy mechanism. The diffusion coefficients of Sn and Sb can be written $D = g \nu a^2 e^{S/k - Q/kT}$ with the attempt frequency $\nu \sim 10^{13} \text{ s}^{-1}$, the jump distance $a = 2.34 \text{ \AA}$ and the geometry+correlation factor g which we assume unity. Kringhøj *et al.*²¹ give the activation energies Q and entropies S for Sn to be 4.8 eV, and $15k$, while those for Sb are 4.1 eV, and $10k$.

Later studies on Ge and self-diffusion via vacancies gave activation energies of 4.86 ± 0.2 and 4.71 ± 0.09 eV, respectively.^{36–38} These results imply that the diffusion of group IV elements is much slower than group V impurities.⁶

The activation energy for SnV diffusion $Q_{\text{SnV}} = E_{\text{SnV}}^{f'} + E_{\text{SnV}}^m$, is the sum of two terms. The first is the formation energy of a vacancy next to Sn assuming that Sn is already grown into the sample and thus $E_{\text{SnV}}^{f'} = E_{\text{SnV}}^f - E_{\text{Sn}}^f = 2.8 - 0.5 \text{ eV} = 2.3 \text{ eV}$ (Table II). $E_{\text{SnV}}^{f'}$ is also the difference between the vacancy formation energy and the binding energy of Sn with a vacancy. The second term is the migration barrier for the SnV center. We now consider the migration/dissociation barrier for SnV.

The migration mechanism of SnV has been considered to the same as PV (E center) notwithstanding the fact that P appears to diffuse via an interstitial mechanism.³⁶ In the E -center mechanism the vacancy travels around a hexagonal ring followed by an exchange of sites with the impurity. In the case of tin this process is modified, because in the initial and final configurations, the tin atom sits at a bond center position, between two vacancies (see Fig. 7). Thus exchange of Sn with either vacancy is an energetically easy process and the dominant step involves V moving to the saddle point between the second and third nearest neighbor positions from a substitutional Sn impurity. However, the entropy factor related to the first diffusion step may be high because it involves correlated move of one Sn and one Si atom.

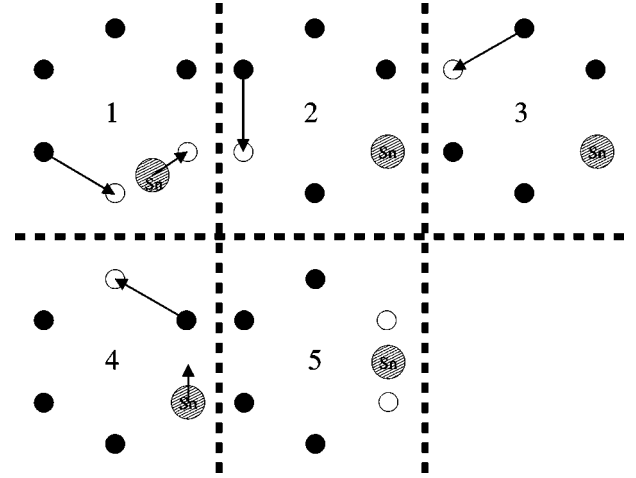


FIG. 7. Mechanism for vacancy assisted diffusion of tin in silicon. The first step differs from the usual E -center mechanism, requiring Sn to move from a site midway between two vacancies, to a vacant site; with a subsequent (or simultaneous) diffusion of the vacancy. During steps 2 and 3, the vacancy jumps to a second and third neighbor site similarly as in the E -center mechanism. The step 4 is the step 1 reversed: the Sn moves back to the D_{3d} position. In the final configuration 5, the SnV has completed one diffusion step.

We have studied the binding energies of the neutral SnV pair at second and third neighbor distances and with the infinite Sn-V separation. The calculations have been carried out using ~ 64 atom supercells using both $2 \times 2 \times 2$ MP sampling and with ~ 216 atomic supercells at the Γ point. The binding energies, with respect to the lowest energy D_{3d} configuration, are 0.6 eV (configuration 1 in Fig. 7), 0.9 eV (configuration 2 in Fig. 7), and 1.2 eV (configuration 3 in Fig. 7). The binding energy when Sn and V are infinitely separated is also found to be 1.2 eV (dropping to 1.0 eV in the 216 atomic supercell) and hence at the third neighbor site the vacancy is essentially free. Thus the vacancy has a high probability of escaping from Sn and wanders through the lattice until trapped by another defect. If this defect is another tin atom, then diffusion of tin can occur by exchange of sites with the vacancy. This explains why reorientation, diffusion and dissociation of SnV have essentially the same barrier equal to 1.2–1.4 eV. Here we have taken into account the migration barrier ≤ 0.2 eV of the vacancy diffusing between the second and third nearest neighbor positions from Sn (the jump indicated by the arrow in configuration 2 or 3 in Fig. 7). The experimental value for the migration barrier of an isolated V is ~ 0.3 eV.²

At ~ 430 K, SnV defects dissociate. The vacancy liberated from tin can then be trapped by a second vacancy, a tin atom, or a nondissociated SnV defect. The calculations show that the binding energies of V with V and SnV are almost identical (Table III rows 2 and 5). This might explain the experiments findings¹⁷ that roughly equal concentrations of V_2^- and SnV_2^- arise from the anneal of SnV above 400 K.

The closeness between the binding energies between neutral Sn and V at third and infinite neighbor sites can be contrasted with PV. With the PV we find the binding energy of 0.6 eV at the third nearest neighbor site and 1.05 eV for an

infinite separation. The difference in energies comes from the Coulomb interaction between the P^+ and V^- when separated at third nearest neighbor sites. In this case we expect reorientation and diffusion via the vacancy mechanism to be much faster than dissociation of PV with less likelihood for the formation of PV_2 defects.

We can now determine the activation energy for diffusion of Sn, Q , which is the sum of the difference in formation energies of 2.3 eV and the migration energy 1.2 or ~ 3.5 eV. The important conclusion is that as the binding energy at third neighbor site, is the same as when completely dissociated, it follows that the diffusion energy is close to that of self-diffusion when mediated by vacancies. The slight lowering in the activation energy is caused by the lowering in the migration barrier of the Sn-bound vacancy when compared to a free vacancy.

Although the diffusion energy is in agreement with the value 3.5 eV found by Akasaka *et al.* and to lesser extent with 4.25 eV by Yeh *et al.*, it is in conflict with the more recent values of 4.8 eV by Kringhøj *et al.*^{19–21} It is difficult to understand how such a high barrier of 4.8 eV can arise from the diffusion of tin caused by SnV. The experimental barriers to reorientation and diffusion of SnV must be both around 1.1–1.4 eV. The weak trapping efficiency of V by Sn can be taken to imply that the reorientation barrier is close to the dissociation barrier—a result also suggested by EPR. These results imply that Q is close to the barrier for self-diffusion mediated by vacancies which has been given to be ~ 3.8 eV in metal diffusion studies,³⁹ or Ge where the barrier is 3.93 eV below 1000 °C but 4.97 eV above.⁴⁰ However, more recent studies on self-diffusion via a vacancy mechanism and for Ge have been carried out and found to give diffusion energies around 4.7–4.9 eV.^{36,38} It is clear that there are in general, and for Sn in particular, there are severe problems in the extraction and interpretation of diffusion barriers.

VI. CONCLUSION

The calculations have resulted in a number of results which are consistent with experiment but there are several areas of disagreement. The assignments for the DK1 and DK2 centers to $(\text{SnV}_2)^-$ and $(\text{SnV}_2a)^-$ seem reliable. The energy of $(\text{SnV}_2b)^-$ is 0.4 eV greater than $(\text{SnV}_2a)^-$ suggesting that the two forms arise through kinetic factors and they are not in equilibrium with each other. The symmetry of the defects and the lack of a spin-density on the Sn atoms are consistent with experiment.¹⁷ For $(\text{SnV}_2)^-$ we find C_1 symmetry in agreement with the experiment, but we argue the symmetry lowering from C_{1h} to C_1 is due to the reconstruction of the dangling Si bonds and not due to the movement of the tin atom across the $\{110\}$ plane.

All the defects are electrically active with deep levels in the gap. The fact that these centers have been detected in EPR demonstrate that they possess deep acceptor levels but their positions have not yet been reported. The Sn-V interaction is found to extend only to the third nearest neighbor distance, which explains that the barriers to reorientation, diffusion and dissociation of SnV are so similar. The binding energy of V with Sn is comparable with oxygen, arsenic, and phosphorus. However, due to the isoelectronicity of Sn and Si, the attraction between Sn and V saturates at third neighbor sites. This implies that the diffusion energy of Sn, calculated to be 3.5 eV—in agreement with some studies—should be close to that of self-diffusion via a vacancy mechanism. This is in agreement with data on self-diffusion derived by metal diffusion studies. However, other experiments on Sn, Ge, and self-diffusion yield values around 4.8 eV. The reasons for these differences are not clear.

ACKNOWLEDGMENTS

R.J. and M.K. thank ENDEASD for support. S.Ö. thanks TFR for financial support. We also thank Arne Nylandsted Larsen and Gerd Weyer for helpful discussions.

¹*Properties of Crystalline Silicon*, edited by R. Hull (The Institution of Electrical Engineers, London, 1999).

²G. D. Watkins, in *Deep Centers in Semiconductors*, 2nd ed., edited by S. T. Pantelides (Gordon and Breach Science Publishers, Switzerland, 1992), Chap. 3.

³B.G. Svensson *et al.*, Phys. Rev. B **43**, 2292 (1991).

⁴S.D. Brotherton, and P.P. Bradley, J. Appl. Phys. **53**, 5720 (1982).

⁵P.M. Fahey, P.B. Griffin, and J.D. Plummer, Rev. Mod. Phys. **61**, 289 (1989).

⁶J. Xie and S.P. Chen, Phys. Rev. Lett. **83**, 1795 (1999).

⁷M. Ramamoorthy and T.P. Pantelides, Phys. Rev. Lett. **76**, 4753 (1996).

⁸M.J. Puska, S. Poykko, M. Pesola, and R.M. Nieminen, Phys. Rev. B **58**, 1318 (1998).

⁹A. Brelot, IEEE Trans. Nucl. Sci. **19**, 220 (1972).

¹⁰A. Brelot, in *Radiation Damage and Defects in Semiconductors, Conference Series No. 16*, edited by J. E. Whitehouse (Institute of Physics, London, 1973), p. 191.

¹¹G.D. Watkins, and J.R. Troxell, Phys. Rev. Lett. **44**, 593 (1980).

¹²G.D. Watkins, Phys. Rev. B **12**, 4383 (1975).

¹³A. Nylandsted Larsen, J.J. Goubet, P. Mejlholm J. Sherman Christensen, M. Fanciulli, H.P. Gunnlaugsson, G. Weyer, J. Wulff Petersen, A. Resende, M. Kaukonen, R. Jones, S. Öberg, P.R. Briddon, B.G. Svensson, J.L. Lindström, and S. Dannefaer, Phys. Rev. B **62**, 4535 (2000).

¹⁴B.J. Coomer, A. Resende, J.P. Goss, R. Jones, S. Öberg, and P.R. Brid don, Physica B **273-4**, 520 (1999).

¹⁵M. Pesola, J. von Boehm, S. Pöykkö, and R.M. Nieminen, Phys. Rev. B **58**, 1106 (1998).

¹⁶E. Simoen *et al.*, Appl. Phys. Lett. **76**, 2838 (2000).

¹⁷M. Fanciulli, and J.R. Byberg, Phys. Rev. B **61**, 2657 (2000).

¹⁸J.S. Nelson, P.A. Schultz, and A.F. Wright, Appl. Phys. Lett. **73**, 247 (1998).

¹⁹Y. Akasaka *et al.*, Jpn. J. Appl. Phys. **13**, 1533 (1974).

²⁰T.H. Yeh, S.M. Hu, and R.H. Kastl, J. Appl. Phys. **39**, 4266 (1968).

²¹P. Kringhøj and A. Nylansted Larsen, Phys. Rev. B **56**, 6396 (1997).

- ²²R. Jones and P. R. Briddon, in *Identification of Defects in Semiconductors*, Vol. 51A of *Semiconductors and Semimetals*, edited by M. Stavola (Academic Press, Boston, 1998), Chap. 6.
- ²³J. Coutinho, R. Jones, P.R. Briddon, and S. Öberg, *Phys. Rev. B* **62**, 10 824 (2000).
- ²⁴G.B. Bachelet, D.R. Hamann, and M. Schlüter, *Phys. Rev. B* **26**, 4199 (1982).
- ²⁵N. Troullier, and J.L. Martins, *Phys. Rev. B* **43**, 1993 (1991).
- ²⁶H.J. Monkhorst and J.D. Pack, *Phys. Rev. B* **13**, 5188 (1976).
- ²⁷N.E. Christensen and M. Methfessel, *Phys. Rev. B* **48**, 5797 (1993).
- ²⁸J.C. Slater, *The Self-Consistent Field for Molecules and Solids* (McGraw-Hill, New York, 1974), Vol. IV.
- ²⁹R.G. Parr and W. Yang *Density-functional Theory of Atoms and Molecules* (Oxford University Press, Oxford, 1989).
- ³⁰H. Zimmermann and H. Rysse, *Appl. Phys. Lett.* **58**, 499 (1991).
- ³¹L.W. Song, X.D. Zhan, B.W. Benson, and G.D. Watkins, *Phys. Rev. B* **42**, 5765 (1990).
- ³²E.Ö. Sveinbjörnsson and O. Engström, *Appl. Phys. Lett.* **61**, 2323 (1992).
- ³³E.Ö. Sveinbjörnsson, G.I. Andersson, and O. Engström, *Phys. Rev. B* **49**, 7801 (1994).
- ³⁴J. Neugebauer and C.G. Van de Walle, *Phys. Rev. B* **50**, 8067 (1994).
- ³⁵Guo-Xin Qian, R.M. Martin, and D.J. Chadi, *Phys. Rev. B* **38**, 7649 (1988).
- ³⁶A. Ural, P.B. Griffin, and J.D. Plummer, *Phys. Rev. Lett.* **83**, 3454 (1999).
- ³⁷M. Sprenger, S.H. Müller, E.G. Sieverts, and C.A.J. Ammerlaan, *Phys. Rev. B* **35**, 1566 (1987).
- ³⁸N. Zangenberg, J. Fage-Pedersen, J. Lundsgaard Hansen, and A. Nylandsted Larsen (unpublished).
- ³⁹H. Bracht, N.A. Stolwijk, and H. Mehrer, *Phys. Rev. B* **52**, 16 542 (1995).
- ⁴⁰A. Hettich, H. Mehrer, and K. Maier, in *Defects and Radiation Effects in Semiconductors*, *IOP Conf. Proc. No. 46*, edited by J. H. Albany (Institute of Physics and Physical Society, London, 1979), p. 500.